



中国气象局地球系统数值预报中心
CMA EARTH SYSTEM MODELING AND PREDICTION CENTRE

Assimilation of FengYun Satellite Data in CMA-GFS Using Advanced Radiative Transfer Modeling System (ARMS)

Fuzhong Weng

CMA Earth System Modeling and Prediction Centre

Presented at 12th Asian Oceania Meteorological User Satellite Conference

Agenda

- **FengYun Satellite Program**
- **CMA Global Forecast Model**
- **Advanced Radiative Transfer Modeling System (ARMS)**
- **Impacts of FengYun Satellite on CMA Forecasts**
- **Summary and Conclusions**

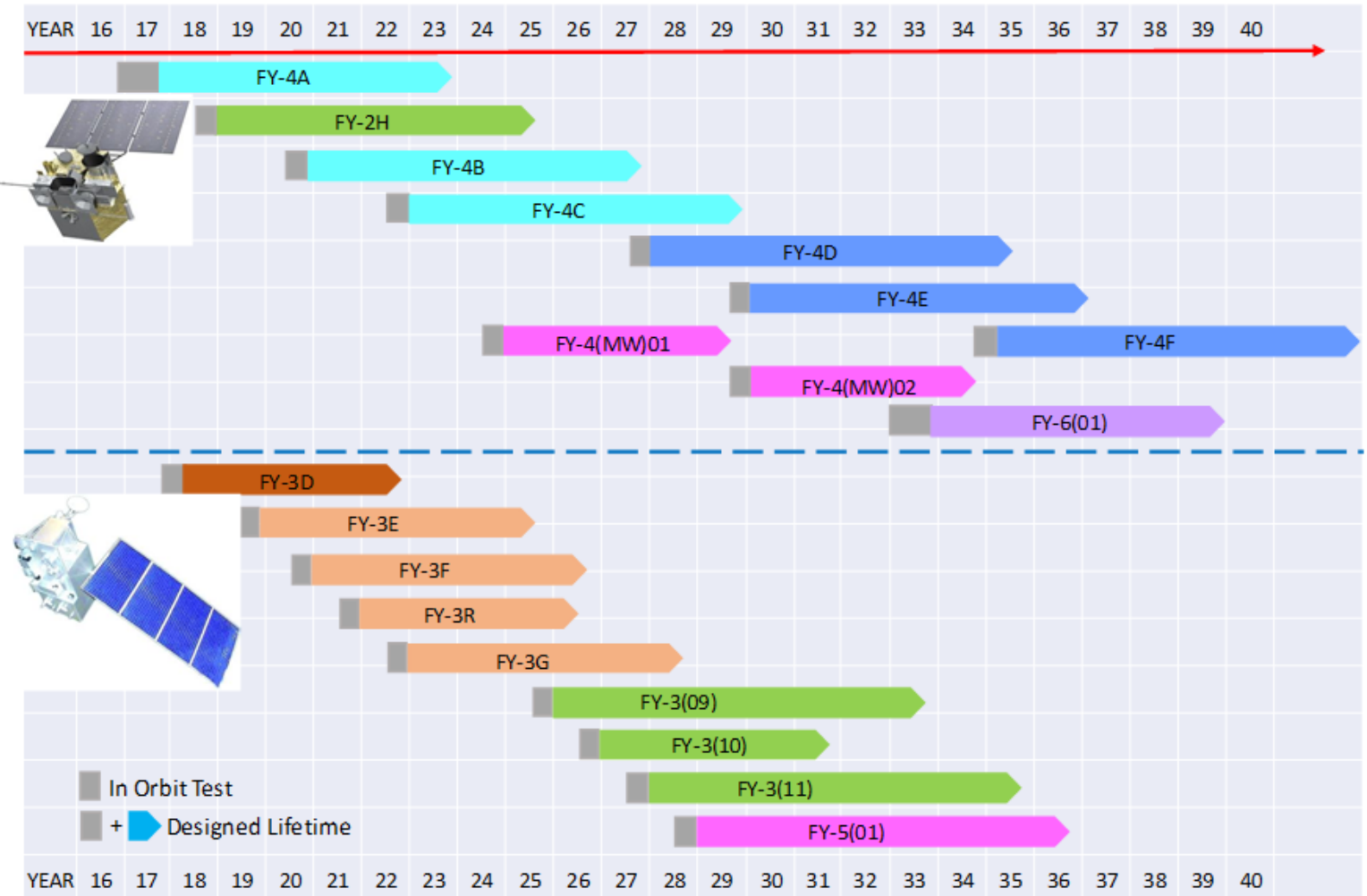
FengYun Satellite Mission

FY-4

- Geostationary Hyperspectral IR sounder
- Geostationary Microwave to Terahertz sounder

FY-3

- Microwave double O₂ bands
- Low light imager
- Precipitation radar
- Ocean Ku/C-band scatterometer
- GNSS ocean reflectometer



CMA NWP Operational Systems

CMA-GFS

- Vertical layer: 87
- Model top: 0.1 hPa, 63 km
- Model resolution: 25 km
- Data assimilation system: 4dvar
- 10 days forecast: 00, 12 UTC
- Five days forecast: 06, 18 UTC

CMA Global Ensemble Prediction System (GEPS)

- Vertical layer: 87
- Model top: 0.1 hPa, 63 km
- Model resolution: 50 km
- 30 members
- 15 days forecast: 00, 12 UTC

CMA Typhoon Model(TYM)

- Belt&Road: 9km
- Lat 15S-60N, Lon: 40-180E
- 5 days forecast
- Four times/day

CMA Regional Forecast System (Meso)

- China: 3km
- 1.5 days forecast
- Eight times/day

CMA Regional Ensemble Prediction System(REPS)

- China: 50km
- 15 members
- 3.5 days forecast (00,12 UTC)

全球中期: 25公里

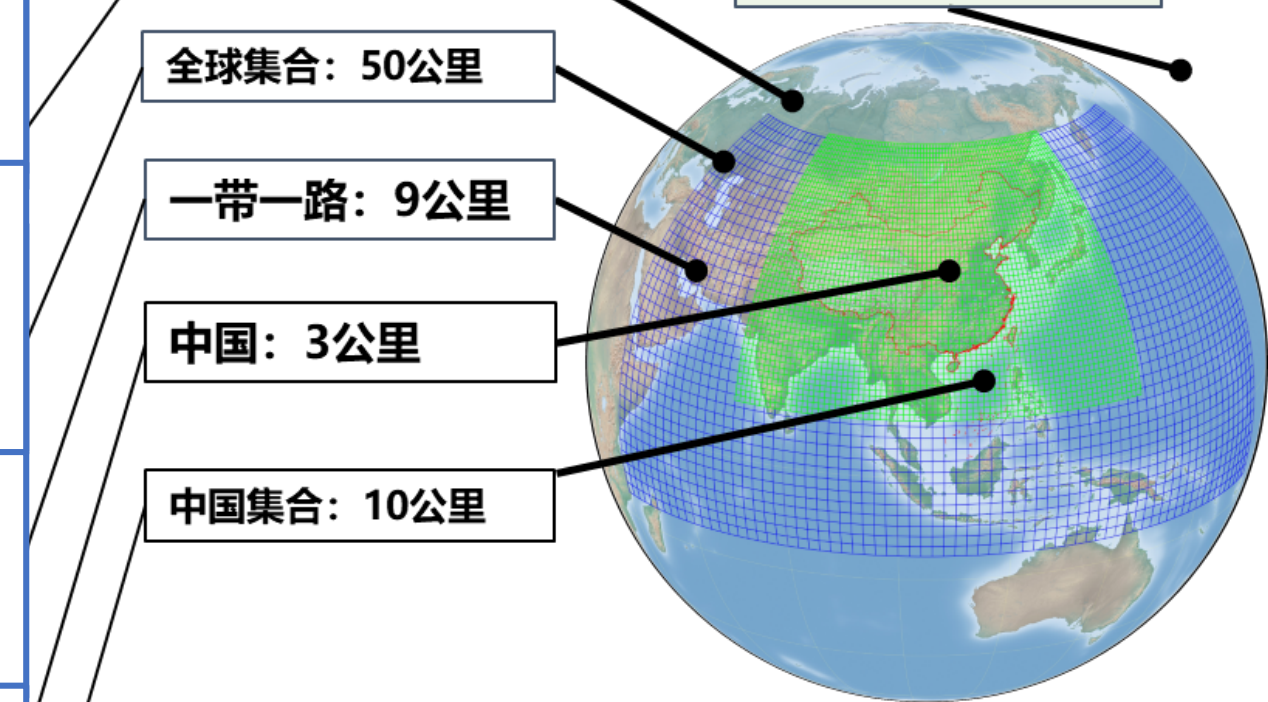
87 levels, 63km

全球集合: 50公里

一带一路: 9公里

中国: 3公里

中国集合: 10公里



Other Models driven by CMA GFS

- Wave Prediction System (00,12 UTC)
- Dust and Haze Warning System (00,12 UTC)
- Emergent Response System for Pollutants Dispersion

CMA 3D/4DVar/ EnKF Data Assimilation Systems

3D or 4D variational algorithms dominate the major NWP centres:

- computationally efficient for what they do
- handles **weak nonlinearities** well

which means "effective at correcting errors when the forward model is weakly nonlinear in the vicinity of the previous forecast"

- well suited for **satellite data assimilation** (radiances)

They are not so good for 'messy' problems:

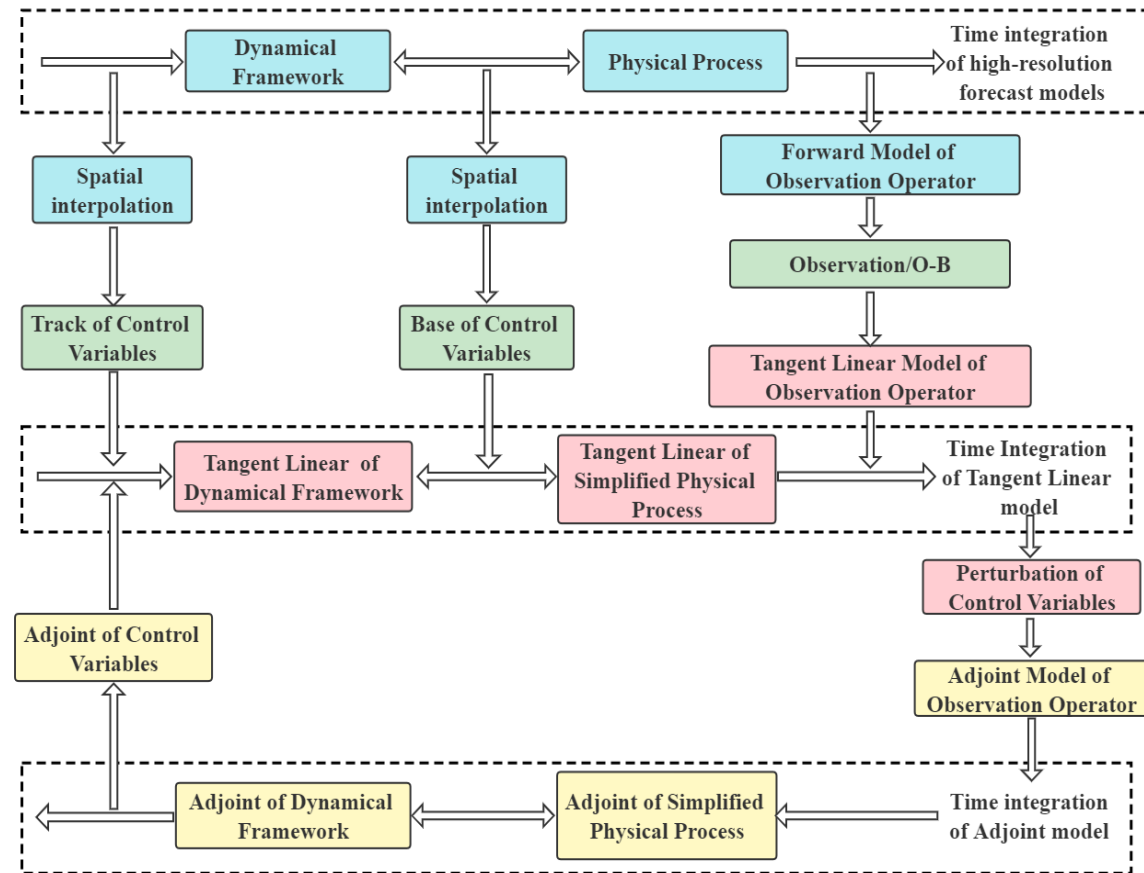
- strong **nonlinearities** (cloudy radiances)
- threshold physics (condensation, precip triggering, rain/snow)
- advection vs discontinuities (surface, fronts, cloud edges)

4D-Var

- is excellent for large-scale dynamics & instabilities (storms),
- copes with arbitrary obs times
- is limited by model & linearization errors
- **numerical cost** limits spatial resolution & time-critical application

Ensemble Kalman Filtering techniques:

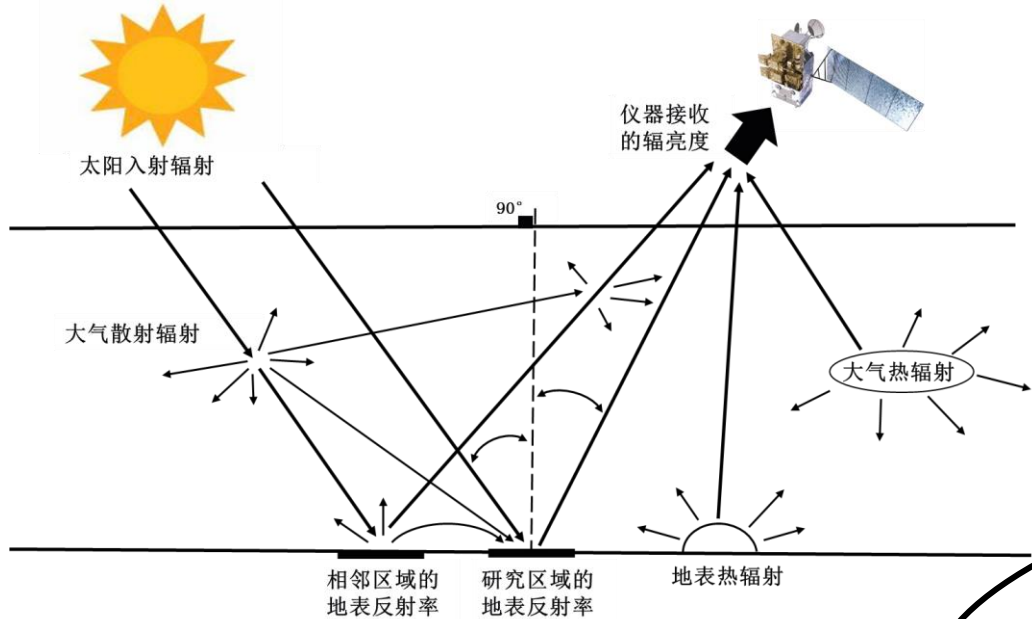
- numerical cost similar to 4D-Var
- good for nonlinearities
- limited by **statistical sampling issues** ("ensemble size")



Satellite Data Assimilation Science Priority

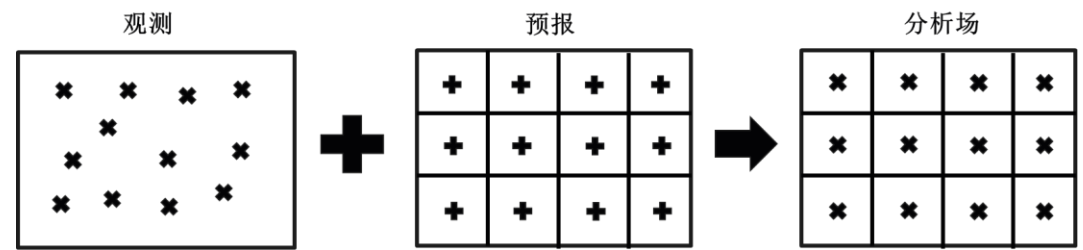
- Prepare for new instruments
- Develop and maintain the observation operators (ARMS, RTTOV)
- Improve uses of aerosol- and clouds-affected radiances
- Improve uses of surface-sensitive channel data
- Achieve uses of satellite data in earth system prediction models

How is Satellite Observation Operator Used in Data Assimilation?



$$\begin{aligned} \mu \frac{d\mathbf{I}(\tau, \mu, \phi)}{d\tau} = & -\mathbf{I}(\tau, \mu, \phi) + \frac{\omega(\tau)}{4\pi} \int_0^{2\pi} \int_{-1}^1 \mathbf{M}(\tau, \mu, \phi; \mu', \phi') \mathbf{I}(\tau, \mu', \phi') d\mu' d\phi' + \\ & + (1-\omega) \mathbf{B} \begin{pmatrix} 1 \\ 0 \\ 0 \\ 0 \end{pmatrix} + \frac{\omega F_0}{4\pi} \exp(-\tau / \mu_0) \begin{pmatrix} M_{11}(\phi, \mu_0, \phi_0) \\ M_{12}(\phi, \mu_0, \phi_0) \\ M_{13}(\phi, \mu_0, \phi_0) \\ M_{14}(\phi, \mu_0, \phi_0) \end{pmatrix} \end{aligned}$$

Satellite observation operator is based on the solution of radiative transfer equation that describes the photons travelling through emitting and scattering earth atmosphere



$$J(\mathbf{x}) = \frac{1}{2} (\mathbf{x} - \mathbf{x}_b)^T \mathbf{B}^{-1} (\mathbf{x} - \mathbf{x}_b) + \frac{1}{2} (\mathbf{H}(\mathbf{x}) - \mathbf{y}^{obs})^T (\mathbf{O} + \mathbf{F})^{-1} (\mathbf{H}(\mathbf{x}) - \mathbf{y}^{obs})$$

$$J(\mathbf{x}_a) = \min_{\mathbf{x}} J(\mathbf{x}) \quad \forall \mathbf{x} \text{ near } \mathbf{x}_b$$

\mathbf{x} – analysis variable

\mathbf{x}_a – final analysis

\mathbf{x}_b – background

\mathbf{B} – background error covariance

\mathbf{y}^{obs} – observations

\mathbf{O} – observation error covariance

\mathbf{H} – observation operator

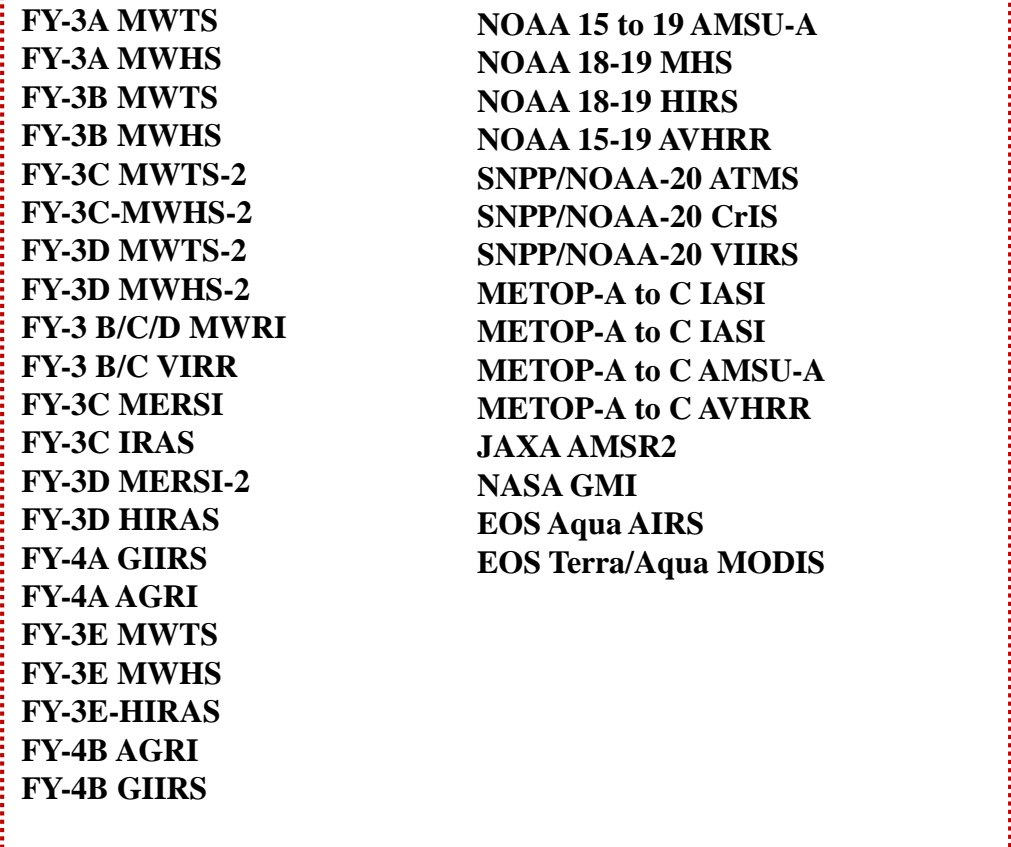
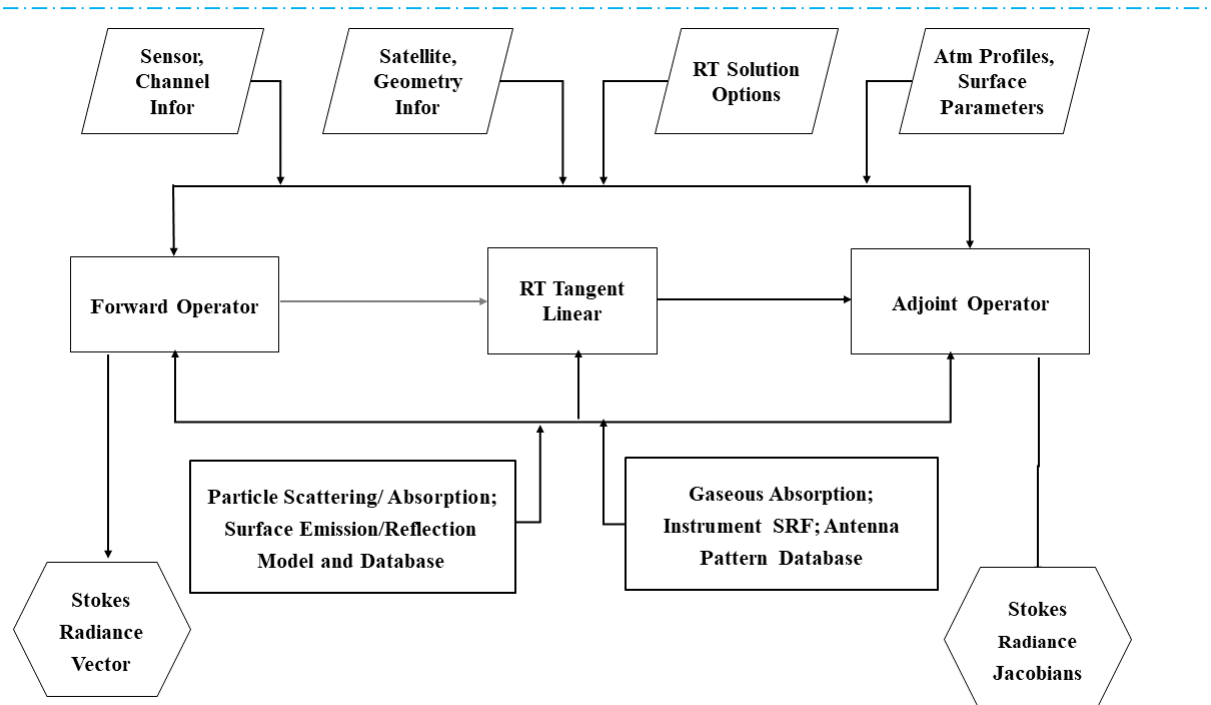
\mathbf{F} – forward model error covariance

The purpose of data assimilation is to define the current states of atmosphere and surface at the NWP model grids from satellite and conventional observations as well as the NWP forecasts. The cost function of J requires the radiative transfer model during the optimization process

Common Issues in Current Fast Radiative Transfer Models Used in NWP Models

- Radiative transfer models have large uncertainties in simulating the radiances in scattering atmospheres (e.g. aerosols, clouds and precipitation).
- Large biases are found at surface sensitive channels over land and behave differently from one model to another.
- Radiative transfer schemes solve only for radiative intensity. The instruments at UV, visible, and microwave wavelengths sensitive to polarization are not well simulated.
- A reference quality ocean emission and reflection model is a gap in our ability to provide absolute calibration of the satellite-based observing systems.

Advanced Radiative Transfer Modeling System (ARMS)



ARMS Special Features:

RT Solver: ADA, P2S, VDISORT

Gas Absorption: SRF integrated absorption coefficients

Scattering LUT: Aerosols-T-matrix, Ice-DDA, Liquid-Mie

Surface Boundary: Emissivity and Reflectivity Matrices

Weng, F., X. Yu, Y. Duan, J. Yang, and J. Wang, 2020: Advanced Radiative Transfer Modeling System (ARMS): A new-generation satellite observation operator developed for numerical weather prediction and remote sensing applications. *Adv. Atmos. Sci.*, 37(2), <https://doi.org/10.1007/s00376-019-9170-2>

ARMS Modular Function

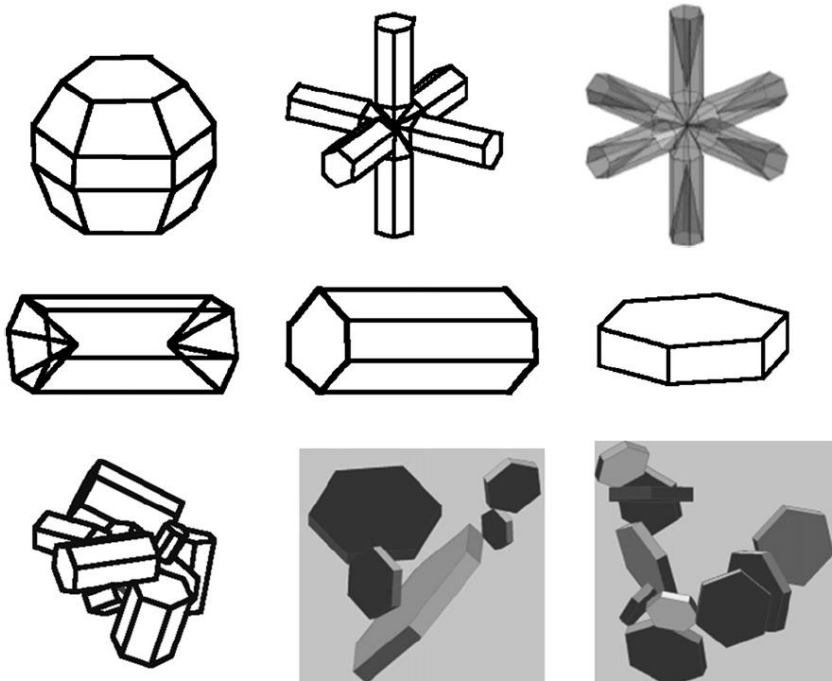
- **Atmospheric gaseous absorption**
 - Band absorption coeff trained by LBL spectroscopy data with sensor response functions
 - Variable gases (e.g. H₂O, CO₂, O₃) .
 - Zeeman splitting effects near 60 GHz
- **Cloud/precipitation scattering and emission**
 - Fast LUT optical models at all phases including non-spherical ice particles
 - Gamma size distributions
- **Aerosol scattering and emission**
 - Types: dust, sea salt, organic/black carbon
 - Lognormal distributions
- **Surface emissivity/reflectivity**
 - Two-scale ocean emissivity and reflectivity model
 - Geometrical optics for infrared ocean emissivity
 - Land microwave emissivity model
 - Land infrared emissivity data bases
- **Radiative transfer schemes**
 - Advanced Doubling and Adding (ADA)
 - Polarized Two Streams (P2S)
 - Vector Discrete Ordinate Radiative Transfer (VDISORT)
 - Tangent Linear and Adjoint

Cloud Optical Property Library Used in ARMS

Ice particle single-scattering property database

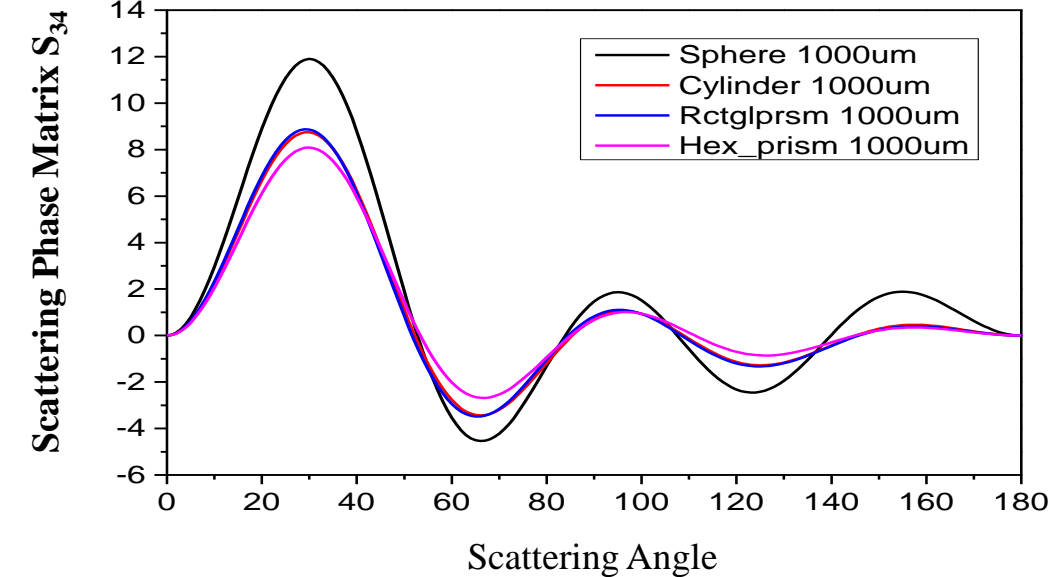
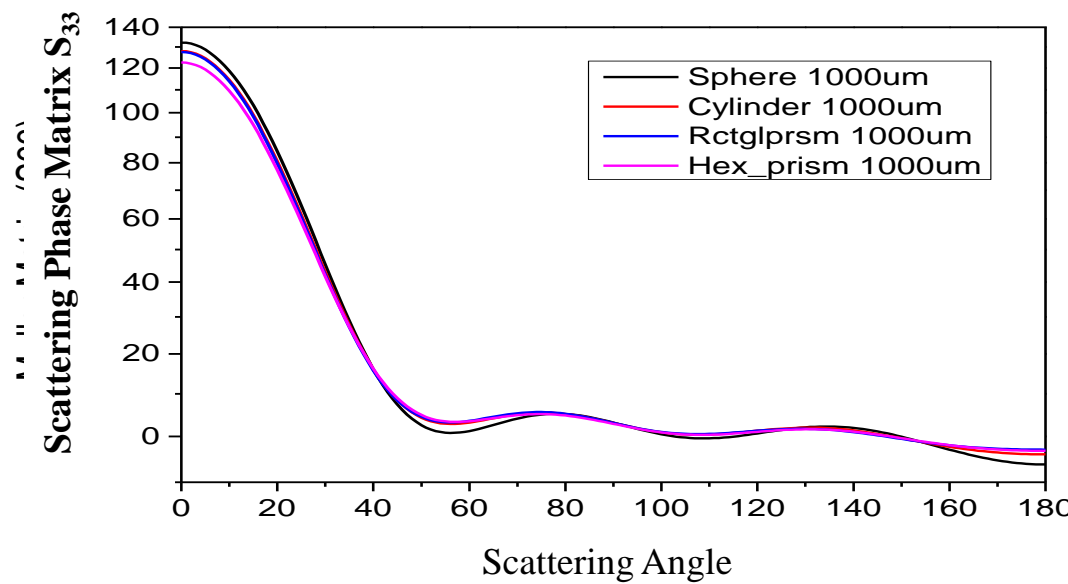
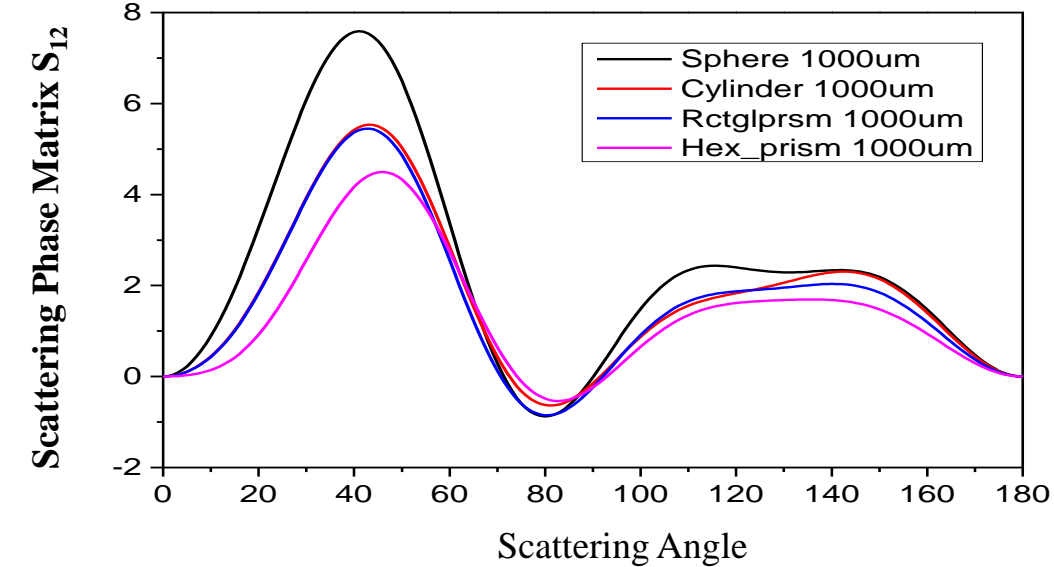
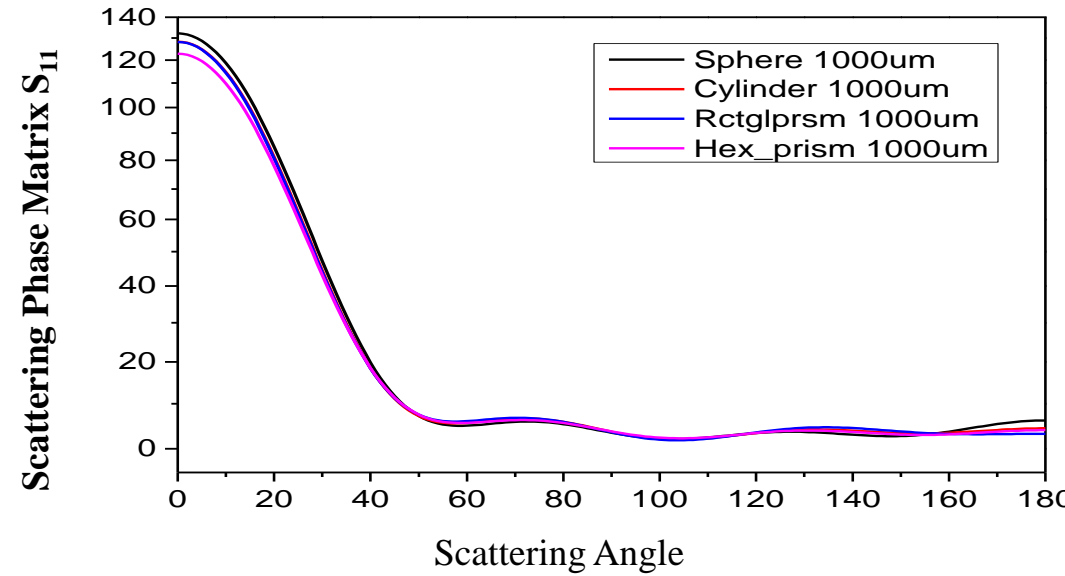
Spectrally Consistent Scattering, Absorption, and Polarization Properties
of Atmospheric Ice Crystals at Wavelengths from 0.2 to 100 μm

PING YANG,* LEI BI,* BRYAN A. BAUM,⁺ KUO-NAN LIOU,[#] GEORGE W. KATTAWAR,[@]
MICHAEL I. MISHCHENKO,[&] AND BENJAMIN COLE*

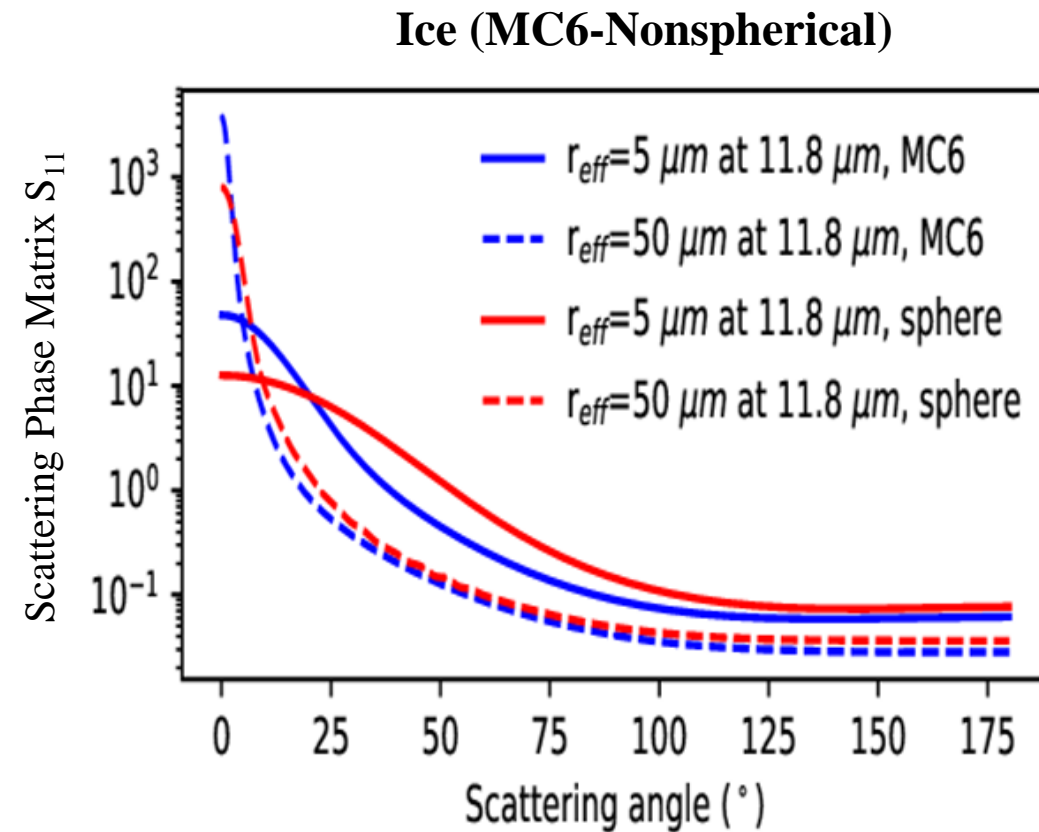
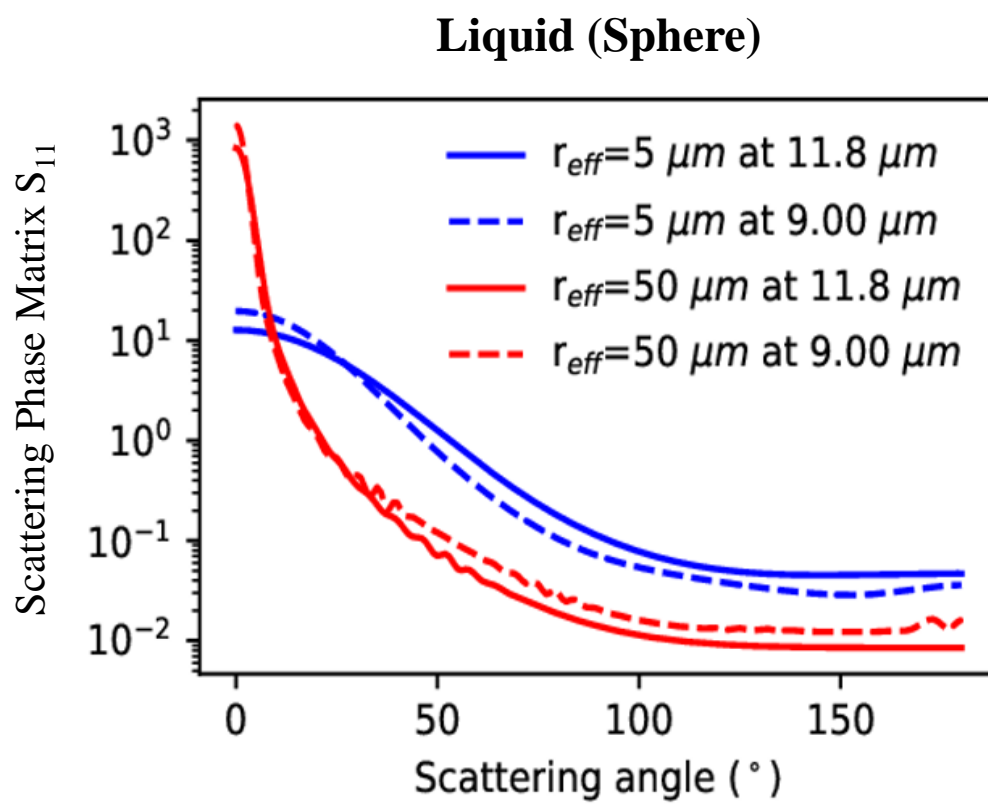


- Developed with the most accurate and state-of-the-art light scattering computation methods (T-Matrix [*Bi et al., 2014*] and IGOM [*Yang et al., 1996*]);
- Wide coverage of the spectrum from 0.2 to 100 μm ;
- Wide particle size range (maximum dimension) from $2\sim 10^4 \mu\text{m}$;
- Complete scattering phase matrix with polarization
- Three degrees of ice surface roughness: Completely Smooth, Moderately Rough, Severely Rough;
- Extended to the microwave spectrum; temperature dependence considered;

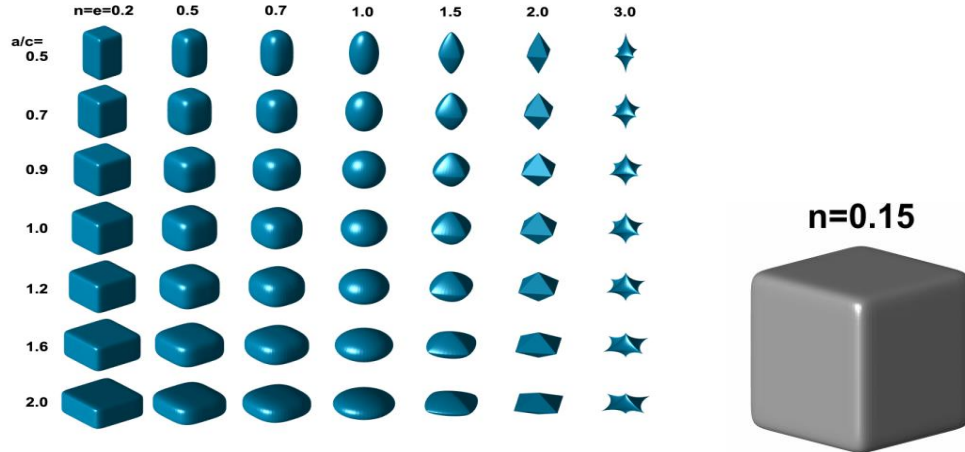
Non-Spherical Particle Scattering at Microwave Frequency



Non-Spherical Scattering at IR Wavelength

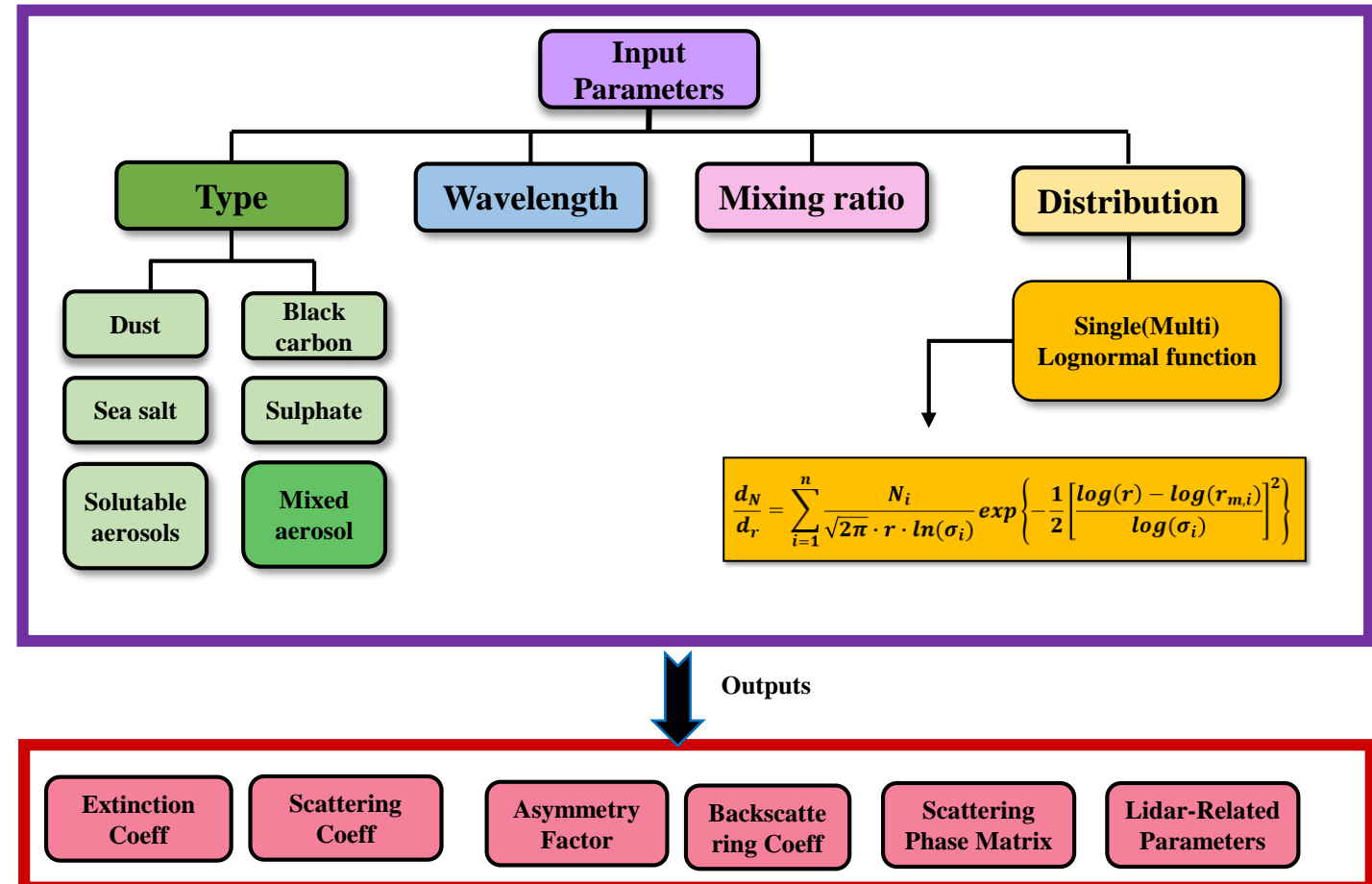


Aerosol Scattering from T-Matrix



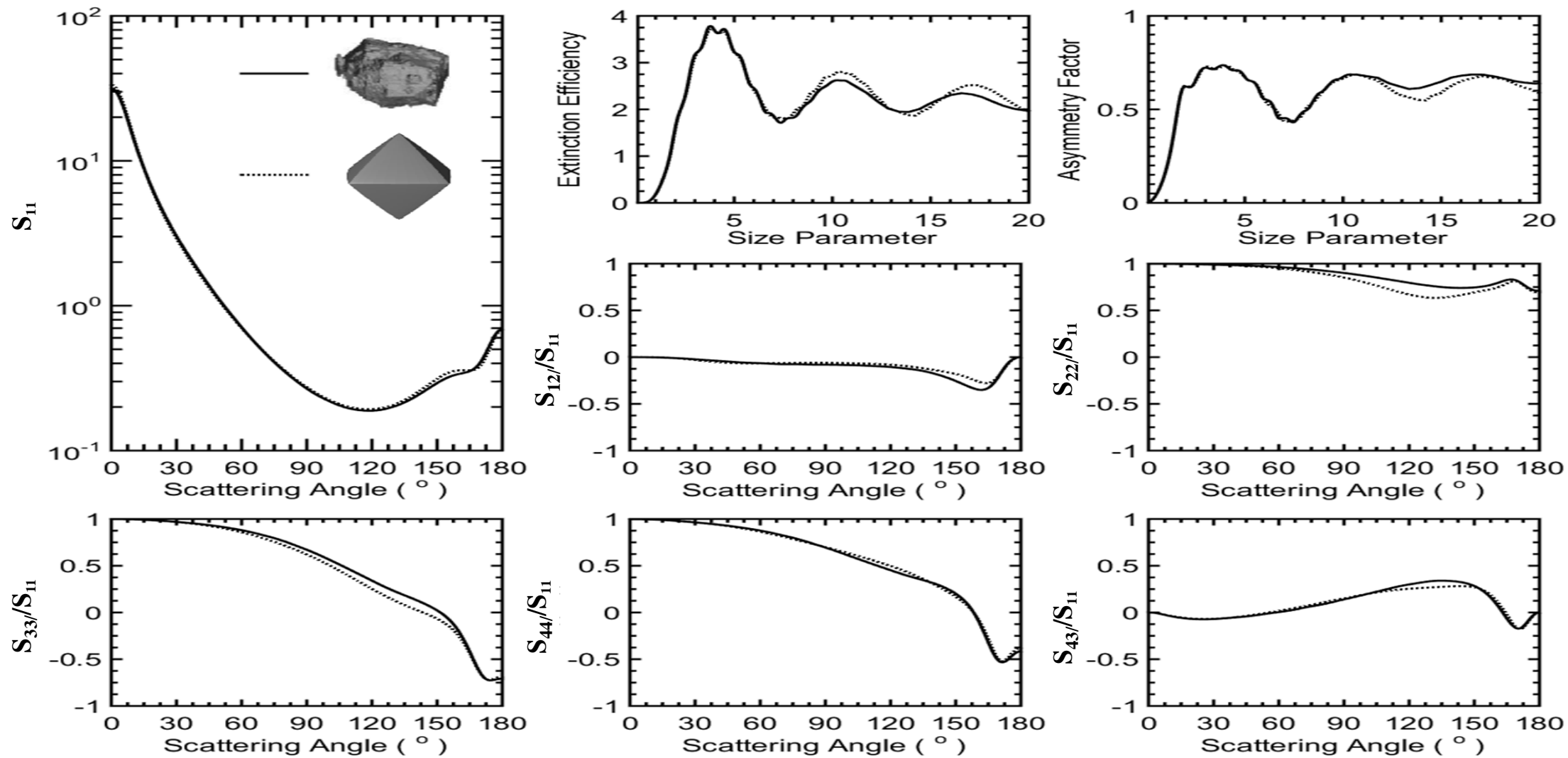
a/c, Particle short and long axis ratio

n, Surface smoothness



Bi et al., 2014, 2020

Aerosol Scattering Database



Vector Radiative Transfer Equation and Its Solution

$$\mu \frac{d\mathbf{I}(\tau, \mu, \phi)}{d\tau} = -\mathbf{I}(\tau, \mu, \phi) + \mathbf{J}(\tau, \mu, \phi) + \mathbf{S}(\tau, \mu, \phi, \mu_0, \phi_0)$$

Extinction

Multiple scattering

Source: single
scattering & thermal
emission

$$\mathbf{I} = [I, Q, U, V]$$

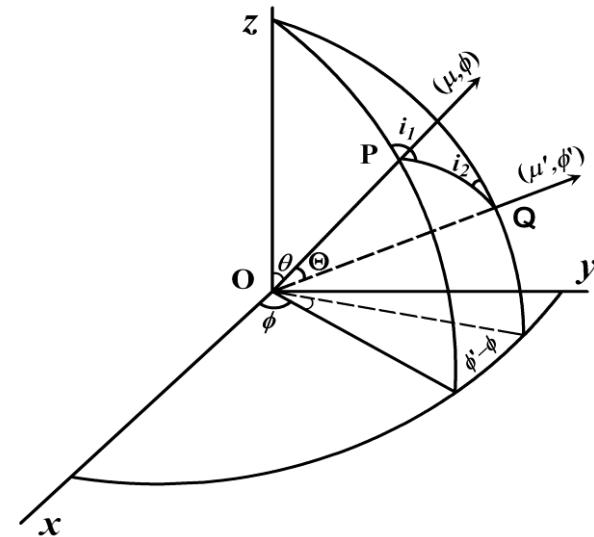
Phase matrix

$$\mathbf{J} = \frac{\omega(\tau)}{4\pi} \int_0^{2\pi} \int_{-1}^1 \mathbf{M}(\tau, \mu, \phi; \mu', \phi') \mathbf{I}(\tau, \mu', \phi') d\mu' d\phi'$$

$$\mathbf{S}(\tau, \mu, \phi, \mu_0, \phi_0) = (1-\omega)B \begin{pmatrix} 1 \\ 0 \\ 0 \\ 0 \end{pmatrix} + \frac{\omega F_0}{4\pi} \exp(-\tau/\mu_0) \begin{pmatrix} M_{11}(\phi, \mu_0, \phi_0) \\ M_{12}(\phi, \mu_0, \phi_0) \\ M_{13}(\phi, \mu_0, \phi_0) \\ M_{14}(\phi, \mu_0, \phi_0) \end{pmatrix}$$

$$\mathbf{M} = \mathbf{L}(\pi - i_2) \mathbf{S}(\Theta) \mathbf{L}(-i_1)$$

$$\mathbf{S} = \begin{bmatrix} S_{11} & S_{12} & S_{13} & S_{14} \\ S_{21} & S_{22} & S_{23} & S_{24} \\ S_{31} & S_{32} & S_{33} & S_{34} \\ S_{41} & S_{42} & S_{43} & S_{44} \end{bmatrix}$$



- Advanced Double and Adding (ADA)
- Polarization Two Stream Approximation (P2S)
- Vector DISORT (VDISORT)
- Line by Line Radiative Transfer Model (LBLRTM)

The scattering phase matrix (or Mueller matrix), \mathbf{S} is defined in the scattering plan (POQ). But the incoming and outgoing radiations are defined in POZ and QOZ plans respectively.

(Weng, JQSRT, 1992 ; Schulz and Weng, JQSRT, 1999)

Lower Boundary Conditions of Radiative Transfer Equation

$$\mathbf{I}(\mu, \phi) = \mathbf{E}\mathbf{S}_t + \frac{1}{\pi} \int_0^{2\pi} \int_0^1 \mathbf{A}(\mu, \phi; -\mu', \phi') \mathbf{I}(-\mu', \phi') \mu' d\mu' d\phi' + \mathbf{A}(\mu, \phi; -\mu_0, \phi_0) \frac{\mu_0 \mathbf{S}_b}{\pi} \exp(-\tau_L / \mu_0)$$

$$\mathbf{I} = [I_l, I_r, U, V] \quad \mathbf{E}(\theta_s, \varphi_s) = \mathbf{I}_i - \int_0^{2\pi} \int_0^1 \mathbf{A} \mathbf{I}_i d\mu' d\phi' \quad \mathbf{I}_i = \begin{pmatrix} 1 \\ 1 \\ 0 \\ 0 \end{pmatrix}$$

$$\mathbf{A} = \begin{pmatrix} A_{vvvv} & A_{vhvh} & \text{Re}(A_{vhvv}) & \text{Im}(A_{vhvv}) \\ A_{hvvh} & A_{hhhh} & \text{Re}(A_{hhhv}) & \text{Im}(A_{hhhv}) \\ 2\text{Re}(A_{vvhv}) & 2\text{Re}(A_{vhhh}) & \text{Re}(A_{vvhv} + A_{vhhv}) & \text{Im}(A_{hhvv} + A_{hvvh}) \\ 2\text{Im}(A_{vvhv}) & 2\text{Im}(A_{vhhh}) & \text{Im}(A_{vvhv} + A_{vhhv}) & \text{Re}(A_{hhvv} - A_{hvvh}) \end{pmatrix}$$

Ocean Reflectivity Matrix from Two-Scale Roughness Theory

$$\mathbf{A} = \begin{pmatrix} A_{vvv} & A_{vhv} & \operatorname{Re}(A_{vhvv}) & \operatorname{Im}(A_{vhvv}) \\ A_{hvvh} & A_{hhh} & \operatorname{Re}(A_{hhvh}) & \operatorname{Im}(A_{hhvh}) \\ 2\operatorname{Re}(A_{vhvh}) & 2\operatorname{Re}(A_{vhvv}) & \operatorname{Re}(A_{vvvh} + A_{vhvh}) & \operatorname{Im}(A_{hhvv} + A_{hvvh}) \\ 2\operatorname{Im}(A_{vhvh}) & 2\operatorname{Im}(A_{vhvv}) & \operatorname{Im}(A_{vvvh} + A_{vhvh}) & \operatorname{Re}(A_{hhvv} - A_{hvvh}) \end{pmatrix}$$

$$\mathbf{A} = \mathbf{A}^c + \langle \mathbf{A}_{SPM}^i \rangle$$

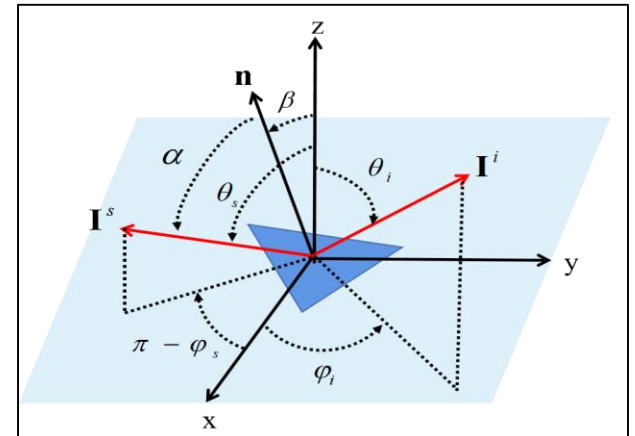
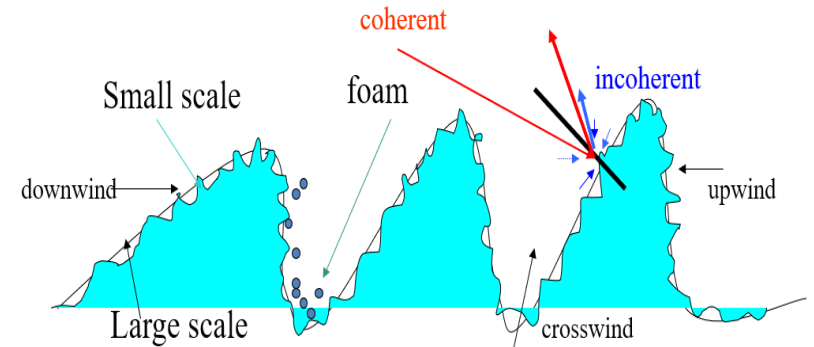
$$\mathbf{A}^c(\theta_i, \varphi_i; \theta_s, \varphi_s) = \frac{P(S_x, S_y)S(\theta_i, \theta_s)}{4\cos\theta_i\cos\theta_s\cos^4\beta} \mathbf{L}(\pi - i_2) \mathbf{R}^c(\theta_{il}, \varphi_{il}; \theta_{sl}, \varphi_{sl}) \mathbf{L}(-i_1)$$

$$P(S_x, S_y) = \frac{F(S_x, S_y)}{2\pi\sigma_u\sigma_c} \exp\left(-\frac{S_x^2}{2\sigma_u^2} - \frac{S_y^2}{2\sigma_c^2}\right)$$

Cox and Munk Ocean Facet pdf

$$\langle \mathbf{A}_{SPM}^i(\theta_i, \varphi_i; \theta_s, \varphi_s) \rangle = \int_{-\infty}^{\infty} dS_y \int_{-\infty}^{\infty} dS_x P(S_x, S_y) S(\theta_i, \theta_s) \mathbf{A}_{SPM}^i(\theta_i, \varphi_i; \theta_s, \varphi_s)$$

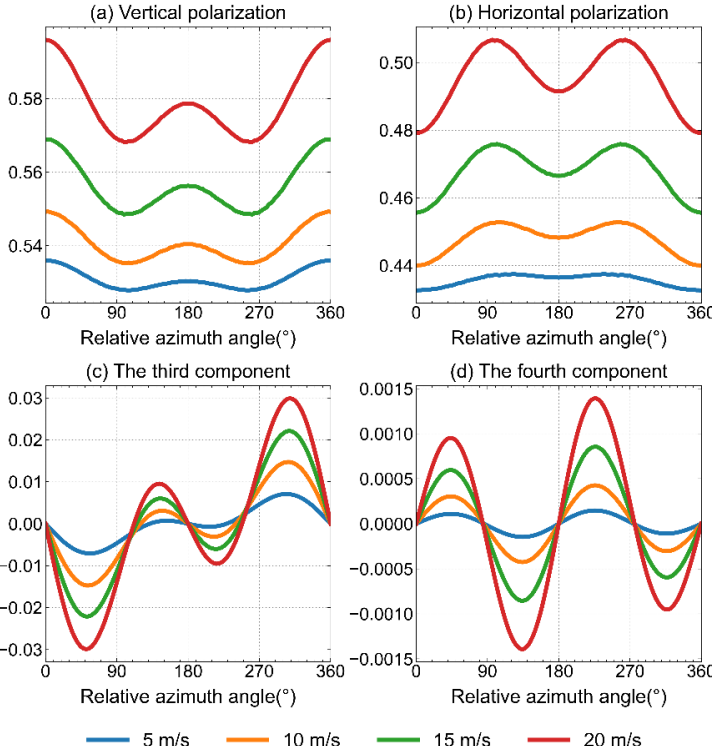
$$\mathbf{A}_{SPM}^i(\theta_i, \varphi_i; \theta_s, \varphi_s) = \mathbf{L}(\alpha_2) \mathbf{R}^i(\theta_{il}, \varphi_{il}; \theta_{sl}, \varphi_{sl}) \mathbf{L}(\alpha_1) k_0^4 \cos\theta_{il} h W_s(k_x, k_y)$$



Major Applications of pBRDF Matrix

Passive

$$\mathbf{E}(\theta_s, \varphi_s) = \mathbf{I}_i - \int_0^{2\pi} \int_0^{\pi/2} \mathbf{A} \cdot \mathbf{I}_i \cos \theta_i \sin \theta_i d\theta_i d\varphi_i$$



Active: monostatic

$$\theta_i = \theta_s, \varphi_i = \varphi_s + \pi$$

$$\sigma_{vv} = 4\pi A_{vvvv} \cos \theta_i \cos \theta_s$$

Active: bistatic

$$\theta_i = \theta_s, \varphi_i = \varphi_s$$

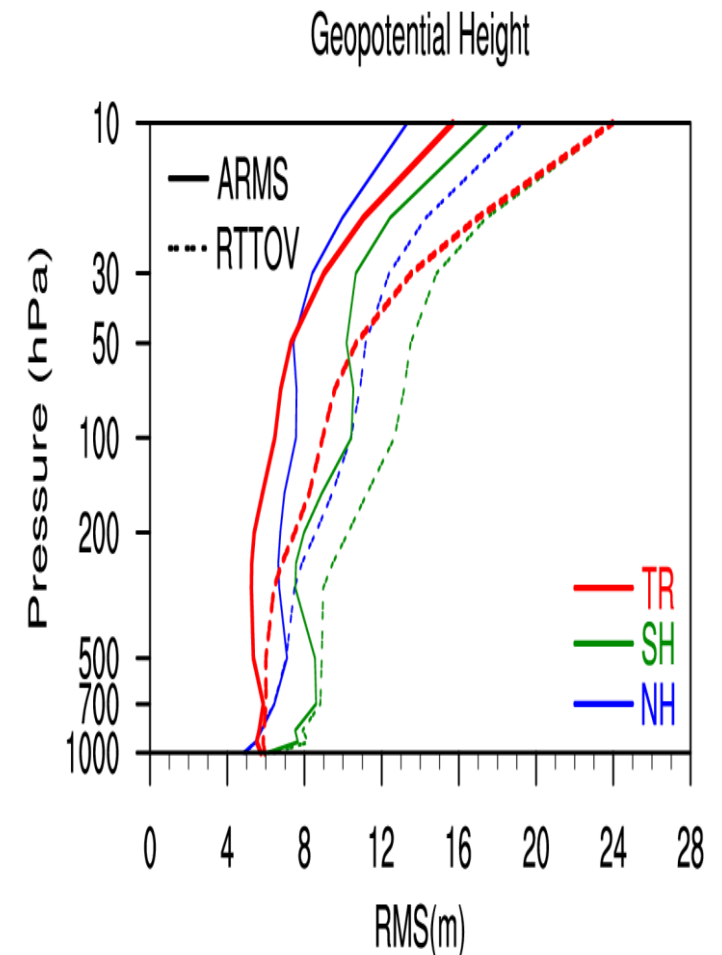
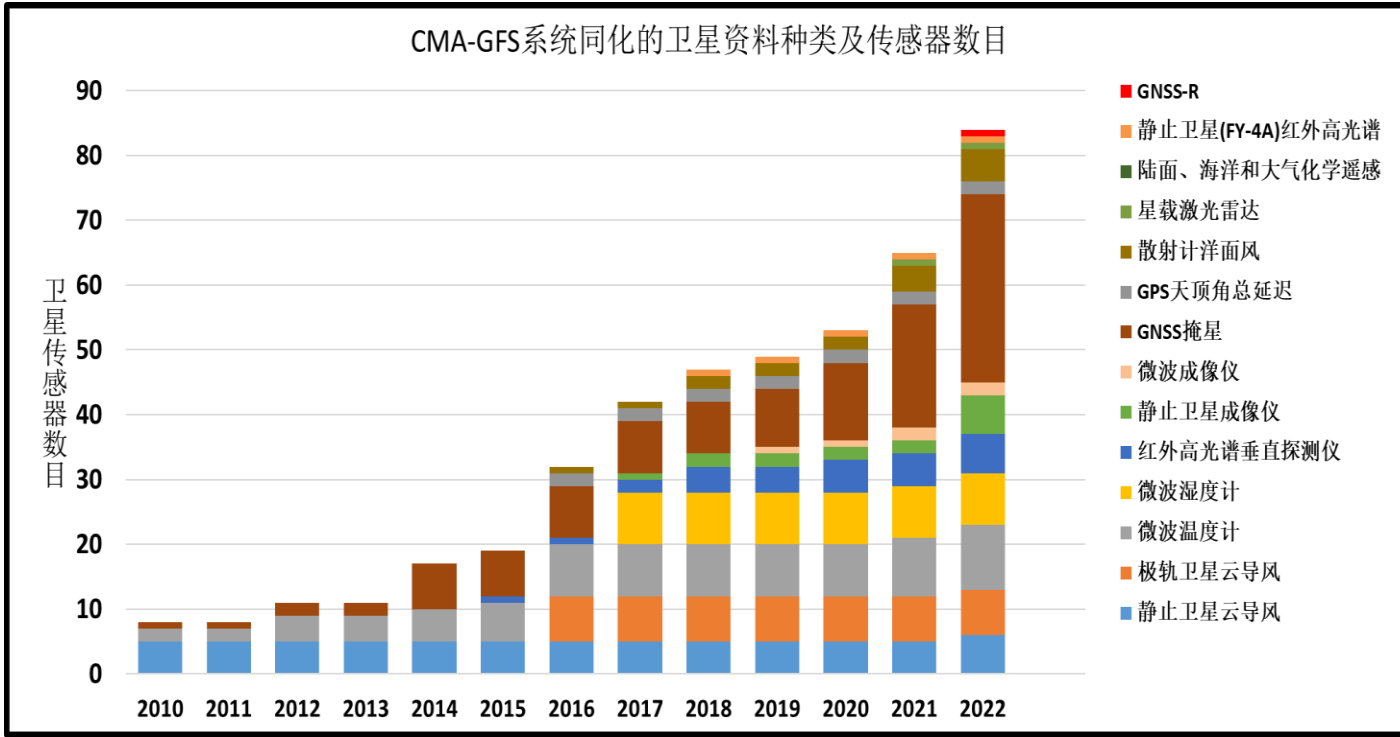
$$\sigma_{vv} = 4\pi A_{vvvv} \cos \theta_i \cos \theta_s$$

SST= 285K, SSS= 35%, frequency=37GHz, $\theta_s = 30^\circ$

X band

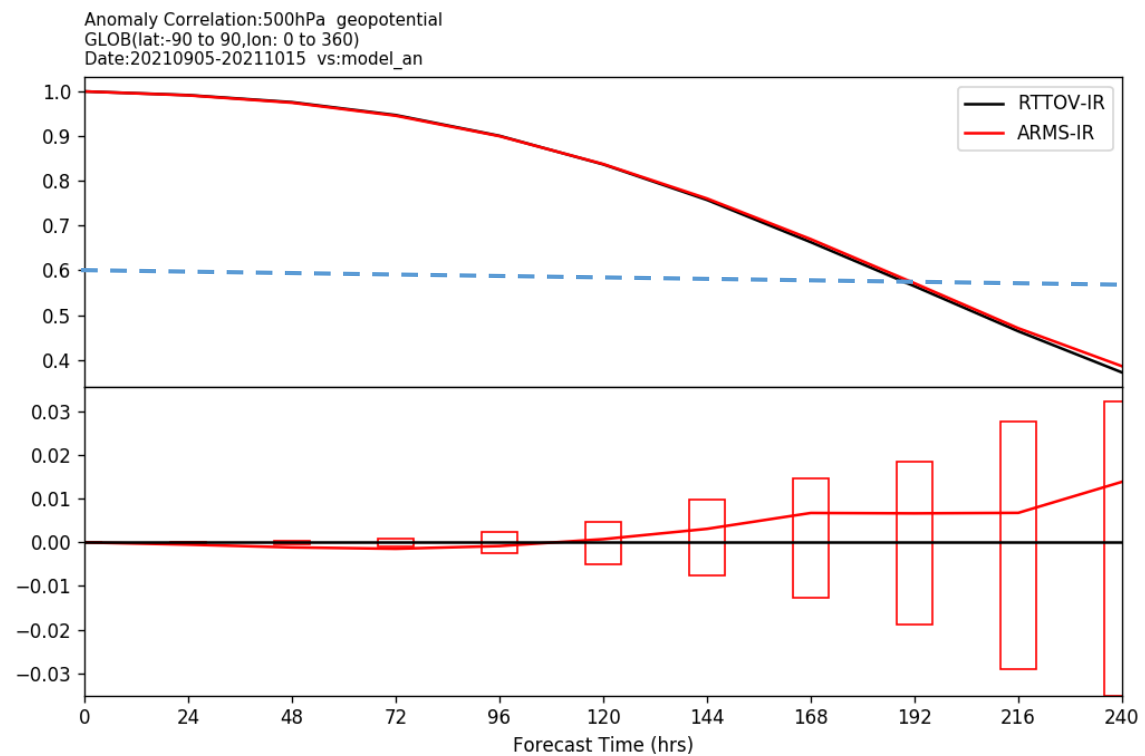
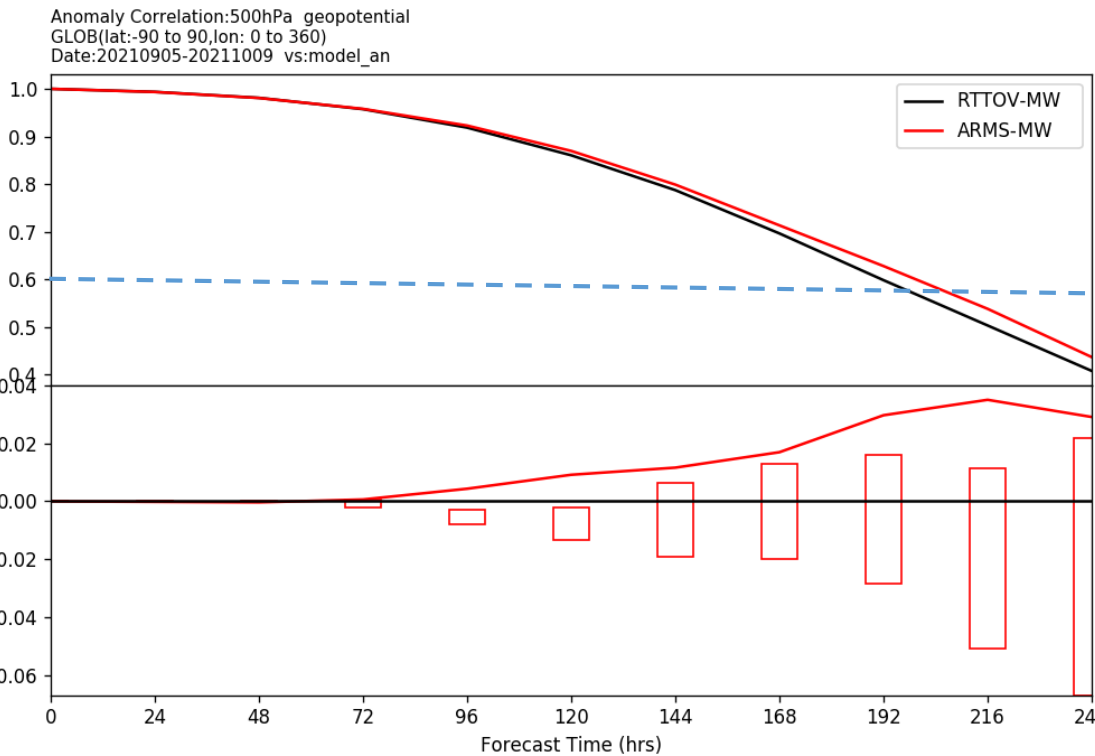
Wind Speed 10m/s

Satellite Data Assimilated in CMA-GFS through ARMS



- ARMS has been successfully integrated into CMA-GFS 4dvar system and is supporting all IR and MW data assimilation.
- ARMS significantly reduces the errors in the analysis field of the geopotential height

Impacts of ARMS in CMA-GFS 4DVAR on ACC at 500 hPa



- 45 days of experiments from 9-1 to 10-15 in 2021.
- For assimilation of microwave sounding data, uses of ARMS can extend the forecasting period by about 4-6 hours in CMA-GFS.
- For assimilation of infrared data, the forecasting scores from ARMS and RTTOV are similar

Summary and Conclusions

- CMA ARMS has its state-of-the art physics and includes many plug-and-play modules and functions allowing for community to contribute its future developments
- ARMS ocean polarized BRDF model has achieved consistent calculations of ocean emissivity, normalized radar cross-section for both active and passive microwave applications
- ARMS has been fully integrated into CMA GFS 4dvar system and is now supporting the assimilation of both infrared and microwave instruments
- Impacts of ARMS on assimilation of microwave data are very positive.